CONF-950816--7

EFFECTS OF WATER CHEMISTRY ON INTERGRANULAR CRACKING OF IRRADIATED AUSTENITIC STAINLESS STEELS*

H. M. Chung, W. E. Ruther, J. E. Sanecki, A. Hins, and T. F. Kassner

Energy Technology Division
Argonne National Laboratory
Argonne, IL 60439

July 1995

To be published in the Proceedings of the Seventh International Symposium on Environmental Degradation of Materials in Nuclear Power Systems - Water Reactors, August 6–10, 1995, Breckenridge, Colorado

*Work supported by the U.S. Nuclear Regulatory Commission, Office of Nuclear Regulatory Research.

Effects of Water Chemistry on Intergranular Cracking of Irradiated Austenitic Stainless Steels*

H. M. Chung, W. E. Ruther, J. E. Sanecki, A. Hins, and T. F. Kassner
Argonne National Laboratory
Argonne, IL 60439, U.S.A.

Abstract

To determine the effects of water chemistry on the susceptibility to irradiation-assisted stress corrosion cracking (IASCC) in austenitic stainless steels, constant-extension-rate tests were conducted in simulated BWR environments on several heats of high- and commercial-purity (HP and CP) Type 304 SS specimens from BWR components irradiated to fluences up to 2.4 x 10^{21} n cm^{-2} (E > 1 MeV). Effects of dissolved oxygen (DO) and electrochemical potential (ECP) in 289°C water were investigated. Dependence of susceptibility to intergranular stress corrosion cracking (IGSCC) on DO was somewhat different for the two materials. Susceptibility of the HP heats, less influenced by DO and ECP, was higher than that of CP material for all DO and fluence levels. Percent IGSCC in the CP material was negligible for DO <0.01 ppm or ECP <-140 mV SHE. Results of analysis by Auger electron spectroscopy indicated that the HP neutron absorber tubes were characterized by relatively lower concentrations of Cr, Ni, and Li and relatively higher concentrations of F and N on grain boundaries than those of the CP materials. It is suggested that a synergism between irradiation-induced grain-boundary Cr depletion and fabrication-related fluorine contamination plays an important role in the stress corrosion cracking behavior of the HP neutron absorber tubes.

Key terms: irradiation-assisted stress corrosion, austenitic stainless steel, water

Introduction

In recent years, failures of reactor-core internal components in both BWRs and PWRs have increased after accumulation of relatively high fluence (>5 x 10^{20} n·cm^{-2}, E >1 MeV). The general pattern of the observed failures indicates that as nuclear plants age and neutron fluence increases, various apparently nonsensitized austenitic stainless steels (SSs) become susceptible to intergranular failure. However, some components (e.g., BWR core shrouds and control blade handles) are known to have cracked under minimal applied stress, low fluence, and negligible thermal sensitization. Although most failed components can be replaced, some safety-significant structural components (e.g., BWR top guides and core plates) would be very difficult or impractical to replace. Therefore, the structural integrity of these components has been a subject of concern, and extensive research has been conducted to provide an understanding of this type of degradation, which is commonly known as irradiation-assisted stress corrosion cracking (IASCC).[1-14]

In general, IASCC is known to be characterized by strong heat-to-heat variation in susceptibility regardless of irradiation condition and material type and grade, even among materials of virtually identical chemical compositions. This seems to cast serious doubt not only on the role of grain-boundary segregation of usual impurities identified in the ASTM specifications, but also on the premise that Cr depletion is the primary mechanism of IASCC. One of the most important factors that has been considered by many investigators to support the Cr-depletion mechanism is the observation that dependence on water chemistry of IGSCC of nonirradiated thermally sensitized material and of IASCC of irradiated solution-annealed material is similar (e.g., see Ref. 1). However, data on the effects of water chemistry of IASCC are limited, and only a few investigations have been reported in the literature for BWR components.[3,4,9] Results from these slow-strain-rate tensile (SSRT) tests appear to indicate that the threshold electrochemical potential (ECP) and dissolved oxygen (DO) necessary to protect against IASCC susceptibility is <-140 mV SHE and <0.01 ppm, respectively, for Type 304 SS components. Results consistent with this have been reported also from uniaxial constant-load tests.[12] However, similar tests on rod tensile specimens, fabricated from a number of commercial- and high-purity (CP and HP) heats of Type 304 and 316 SS and irradiated in a BWR, indicated significant heat-to-

*Work supported by the U.S. Nuclear Regulatory Commission, Office of Nuclear Regulatory Research.

heat variations not only in IASCC susceptibility but also in response to water chemistry.[7] We reported previously a similar behavior in BWR components fabricated from several HP and CP heats of Type 304 SS for a fixed condition of water chemistry, i.e., DO of ≈0.3 ppm and ECP of ≈60–150 mV SHE.[5,6] In this study, effects of water chemistry were investigated for wider ranges of DO and ECP. The objective was twofold: (1) to better define the effects of water chemistry on susceptibility of the HP and CP Type 304 SS BWR components, thereby providing an independent confirmation of the protection potential, and (2) to provide an insight as to the origin of the significant heat-to-heat variation in susceptibility to IASCC.

Experimental Procedures

Materials and Irradiation

A description and procedures for hot-cell SSRT tests were given in a previous report.[5] Cylindrical SSRT specimens 89 mm long were sectioned from top-, middle-, and bottom-axial positions of the BWR neutron absorber rods listed in Table 1. Sheet tensile specimens fabricated from BWR control blade sheaths were also tested. The fast neutron fluence and chemical composition of the HP and CP heats of Type 304 SS are given in Table 1.

SSRT Test

SSRT tests were conducted in air (Table 2) and in simulated BWR water (Tables 3–5) at 289°C at a fixed strain rate of 1.65×10^{-7} s^{-1}. SSRT tests in water were conducted at DO concentrations of ≈8 ppm (Table 3), ≈0.3 ppm (Table 4), and ≈0.001 ppm (Table 5). Dissolved oxygen content in water was controlled by purging with nitrogen gas and was measured on the effluent side. Effluent ECP values were determined by sequential measurements on working electrodes of Type 304 SS and platinum. When the stainless steel ECP was stabilized, the SSRT test was initiated. During the test, ECP was measured periodically until the specimen fractured. For each SSRT test conducted, the values of DO, average ECP, conductivity, and pH of water are listed in Tables 3–5.

Table 1. Chemical composition (in wt.%) and fluence of high- and commercial-purity Type 304 SS BWR components.

Heat ID No.	Cr	Ni	Mn	C	N	B	Si	P	S	Source Code	Service Reactor	Fluence (10^{21} n/cm^2)
HP304-A	18.50	9.45	1.53	0.018	0.100	<0.001	<0.03	0.005	0.003	NAT[a]	BWR-B	0.2-1.4
HP304-B	18.30	9.75	1.32	0.015	0.080	<0.001	0.05	0.005	0.005	NAT[a]	BWR-B	0.2-1.4
HP304-CD	18.58	9.44	1.22	0.017	0.037	0.001	0.02	0.002	0.003	NAT[a]	BWR-B	0.2-1.4
HP304-CD	18.58	9.44	1.22	0.017	0.037	0.001	0.02	0.002	0.003	NAT[a]	BWR-QC	2.0
CP304-A	16.80	8.77	1.65	0.08[b]	0.052	–	1.55	0.045[b]	0.030[b]	NAT[c]	BWR-Y	0.2-2.0
CP304-B	18-20	8-10.5	2.00[b]	0.08[b]	–	–	1.00[b]	0.045[b]	0.030[b]	CBS[d]	BWR-LC	0.5-2.6

[a]High-purity neutron absorber tubes, OD = 4.78 mm, wall thickness = 0.63 mm, composition before irradiation.
[b]Represents maximum value in the specification; actual value not measured.
[c]Commercial-purity absorber tubes, OD = 4.78 mm, wall thickness = 0.79 mm, composition after irradiation.
[d]Commercial-purity control blade sheath, thickness 1.22 mm, actual composition not measured.

Post-Test Examination

The fracture surfaces of SSRT specimens were analyzed by scanning electron microscopy (SEM) to determine quantitatively the fractions of transgranular and intergranular fracture morphologies (%IGSCC). Grain-boundary microchemistry was analyzed with a JEOL Company JAMP-10 Model scanning Auger microscope (SAM) on specimens charged with hydrogen and fractured in-situ in the ultrahigh vacuum of the SAM.[5,6]

Results

Total Elongation

On the basis of the data in Tables 3–5, %IGSCC determined from SEM fractography has been plotted in Fig. 1 as a function of total elongation in water. The figure shows that uniaxial ductility in water is an approximate measure of susceptibility to IGSCC (or vice

Table 2. Results of Tensile Test[a] in Air on Irradiated Type 304 SS BWR Core-Internal Components at 289°C

Specimen Ident. No.	Hot-cell Ident. No.	Source Heat[b] Ident. No.	Fast-Neutron Fluence, $n \cdot cm^{-2}$	SSRT No.	Tensile Properties				
					Failure Time, h	Max. Stress, MPa	Yield Stress, MPa	Total Elong., %	%IG %
BL-BWR-2H	389E3A	CP304-A	2.0×10^{21}	IR-9	228	631	595	13.5	0
BL-BWR-2M	389E2D	CP304-A	0.6×10^{21}	IR-3	580	465	221	34.8	0
BL-BWR-2L	389E1A	CP304-A	0.2×10^{21}	IR-2	260	390	184	15.6	0
VH-A7A-L2	406A1F	HP304-A	1.4×10^{21}	IR-5	93	786	702	5.6	0
VM-D5B-L2	406C3	HP304-CD	0.7×10^{21}	IR-6	405	684	591	24.2	0
VL-A4C-L2	406B3	HP304-A	0.2×10^{21}	IR-10	231	607	460	13.7	0
C71U	LSC-1	CP304-B	2.45×10^{21}	IR-15	123	830	820	7.3	0
C72T	LCS-4	CP304-B	2.54×10^{21}	IR-13	121	876	815	7.2	0
C7T1T	LSC-7	CP304-B	1.59×10^{21}	IR-19	203	792	666	12.0	0
C7T1M7	LCS-9	CP304-B	1.17×10^{21}	IR-21	136	777	736	7.5	0
C7M2K	LSC-11	CP304-B	0.53×10^{21}	IR-23	361	644	570	21.4	0
C7B1W	LCS-5	CP304-B	0.23×10^{21}	IR-17	574	577	360	34.1	0

[a]Test in air at 289°C and strain rate of 1.65×10^{-7} s^{-1}.

Table 3, SSRT[a] Test Results on Irradiated High- and Commercial-Purity Type 304 SS BWR Neutron Absorber Tubes in High-Purity Water Containing ≈8 ppm Dissolved Oxygen at 289°C

Source Heat Ident. No.	Fast-Neutron Fluence, $n\ cm^{-2}$	Hot Cell Ident. No.	Swagelok Ident. No.	SSRT No.	Feedwater Chemistry				SSRT Parameters				
					Oxygen Conc., ppm	Average ECP mV SHE	Cond. at 25°C μScm^{-1}	pH at 25°C	Failure Time, h	Max. Stress, MPa	Total Elong., %	TGSCC %	IGSCC %
HP304-A	1.4×10^{21}	A6A2-1	32	IR-41	8.3	+156	0.120	6.35	31.9	414	1.90	2	56
HP304-A	1.4×10^{21}	A6A2-2	33	IR-42	8.2	+267	0.118	6.48	31.9	372	1.89	3	68
HP304-B	1.4×10^{21}	473A-1	47	IR-43	8.9	+165	0.118	6.49	31.8	453	1.88	0	59
HP304-CD	1.4×10^{21}	473C-1	42	IR-44	8.2	+122	0.084	6.80	29.2	360	1.73	3	62
HP304-B	0.7×10^{21}	473D-1	38	IR-53	8.2	+155	0.119	6.49	55.8	445	3.3	0	31
CP304-A	0.2×10^{21}	389C1-1	28	IR-51	8.04	+164	0.098	6.09	153.0	310	9.1	47	0
CP304-A	0.6×10^{21}	389C2-1	20	IR-45	8.2	+131	0.083	6.80	154.3	359	9.2	55	2
CP304-A	2.0×10^{21}	389C3-2	27	IR-52	7.9	+178	0.066	7.06	43.5	390	2.6	3	52

[a]Strain rate of 1.65×10^{-7} s^{-1}.

Table 4. SSRT[a] Test Results on Irradiated Type 304 SS BWR Core-Internal Components in Simulated BWR Water Containing ≈0.3 ppm Dissolved Water at 289°C

Specimen Ident. No.	Hot-cell Ident. No.	Source Heat Ident. No.	Fast-Neutron Fluence, $n \cdot cm^{-2}$	SSRT No.	Feedwater Chemistry: Oxygen Conc., ppm	Feedwater Chemistry: Average ECP, mV SHE	Feedwater Chemistry: Cond. at 25°C, $\mu S \cdot cm^{-1}$	Feedwater Chemistry: pH at 25°C	SSRT Parameters: Failure Time, h	SSRT Parameters: Max. Stress, MPa	SSRT Parameters: Total Elong., %	SSRT Parameters: TGSCC, %	SSRT Parameters: IGSCC, %
BL-BWR-2H	389E3D	CP304-A	2.0×10^{21}	IR-12	0.30	90	0.13	6.27	21	415	1.2	8	28
BL-BWR-2M	389E2A	CP304-A	0.6×10^{21}	IR-8	0.29	76	0.15	6.32	140	359	8.3	55	0
BL-BWR-2L	389E1D	CP304-A	0.2×10^{21}	IR-1	0.28	115	0.13	6.23	107	337	6.7	43	0
VH-A7A-L1	406A1E	HP304-A	1.4×10^{21}	IR-4	0.28	106	0.10	6.28	11	417	0.6	2	58
VM-D5B-L1	406C2	HP304-CD	0.7×10^{21}	IR-7	0.28	148	0.12	6.26	31	552	1.8	8	34
VL-A4C-L1	406B2	HP304-A	0.2×10^{21}	IR-11	0.33	88	0.14	6.33	77	520	4.6	47	14
C71X	LSC-2	CP304-B	2.26×10^{21}	IR-16	0.31	82	0.12	6.23	74	841	4.2	2	3
C72S	LCS-3	CP304-B	2.64×10^{21}	IR-14	0.32	59	0.11	6.25	84	843	5.0	2	4
C7T1J	LCS-8	CP304-B	1.53×10^{21}	IR-20	0.36	102	0.11	6.22	101	872	6.1	3	6
C7T1M8	LSC-10	CP304-B	1.15×10^{21}	IR-22	0.36	–	0.11	6.28	79	815	4.7	5	4
C7M2L	LCS-12	CP304-B	0.50×10^{21}	IR-24	0.32	–	0.08	6.38	290	657	18.1	0	0
C7B1X	LSC-6	CP304-B	0.20×10^{21}	IR-18	0.31	–	0.11	6.24	457	572	27.1	8	0

[a]Strain rate of 1.65×10^{-7} s^{-1}.

Table 5. SSRT[a] Test Results on Irradiated High- and Comercial-Purity Type 304 SS BWR Neutron Absorber Tubes in High-Purity Water Containing ≈0.001 ppm Dissolved Oxygen at 289°C

Source Heat Ident. No.	Fast-Neutron Fluence, $n \cdot cm^{-2}$	Hot Cell Ident. No.	Swagelok Ident. No.	SSRT No.	Feedwater Chemistry: Oxygen Conc., ppm	Feedwater Chemistry: Average ECP mV SHE	Feedwater Chemistry: Cond. at 25°C $\mu S \cdot cm^{-1}$	Feedwater Chemistry: pH at 25°C	SSRT Parameters: Failure Time, h	SSRT Parameters: Max. Stress, MPa	SSRT Parameters: Total Elong., %	SSRT Parameters: TGSCC %	SSRT Parameters: IGSCC %
HP304-CD	1.4×10^{21}	473C-2	43	IR-55	0.001	–413	0.062	7.20	95.2	740	5.7	10	7
HP304-B	1.4×10^{21}	473A-2	48	IR-54	0.001	–567	0.062	7.20	103.1	773	6.1	8	6
HP304-CD	1.4×10^{21}	473B-1	44	IR-56	<0.003	–319	0.061	7.47	66.4	717	3.9	7	15
CP304-A	2.0×10^{21}	389F3-1	40	IR-58	0.001	–596	0.063	7.20	215.4	627	12.8	42	0
CP304-A	2.0×10^{21}	389F3-2	39	IR-59	0.001	–572	0.061	7.18	202.2	615	12.4	24	0

[a]Strain rate of 1.65×10^{-7} s^{-1}.

versa) regardless of water chemistry. However, results of the present investigation indicate that for a comparable ductility, susceptibility to intergranular cracking is somewhat lower than those obtained for BWR dry tubes.[2,4,9]

Intergranular fracture morphology was observed only in specimens fractured in water; %IGSCC was always zero for SSRT tests in air (Table 2). Nonductile fracture surface morphology resembling dislocation-channel-induced fracture was observed frequently in thin layers beneath the surface oxide in both air or water. This type of fracture will influence crack nucleation but is believed irrelevant to the key process of intergranular cracking. This signifies the importance of the role of water as a corrosive environment in sustaining the grain-boundary separation.

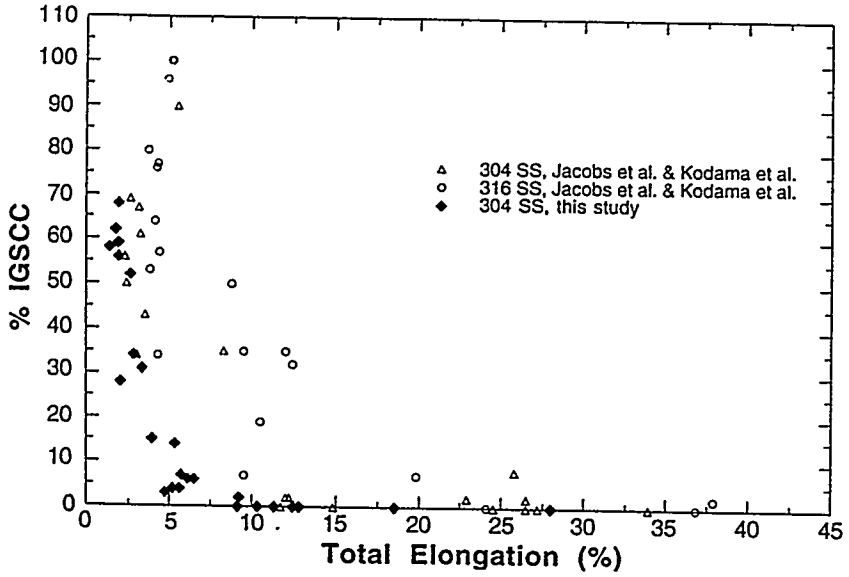

Figure 1.

Comparison of total elongation vs. %IGSCC of BWR components, fabricated from Type 304 and 316 SS, determined in this and other investigations.

Susceptibility to IGSCC

In Fig. 2, effects of DO on %IGSCC vs. fluence are shown for the HP (HP304-A, B, and CD) and CP neutron absorber tubes tested in this study. Susceptibility of the control blade sheath (fabricated from another CP-grade heat) to IGSCC was negligible for all fluence levels; therefore, no tests were conducted to investigate the effect of DO levels other than ≈0.3 ppm. Percent IGSCC vs. DO (in the range of 0.02 to 32 ppm) for CP Type 304 SS dry tubes, reported by Kodama et al.,[3,4] is also shown in the figure for comparison. The strong effects of DO on the susceptibilities of the CP Type 304 SS BWR neutron absorber and dry tubes appear to be quite similar.

However, DO dependence of the neutron absorber tubes fabricated from the HP heats appears to be different in several ways from those of the tubes fabricated from the CP material: for comparable fluence levels, susceptibility of the former materials to IGSCC seems to be less dependent on DO than is the latter material; furthermore, some degree of susceptibility to IGSCC was observed in the HP materials even at the very low DO of ≈0.001 ppm. Susceptibility of the HP materials was significantly higher than that of CP materials regardless of either DO or fluence. A similar trend is also obvious from Fig. 3, in which the effect of ECP on %IGSCC is shown. In the figure, results obtained for CP 304 SS by Indig et al.[3] agree well with those from the present investigation, whereas HP tubes exhibit distinct cracking behavior less sensitive to ECP than the CP materials.

Crack Growth Rate

Approximate intergranular crack growth rate (IGCGR) was estimated from SSRT data by a procedure similar to that of Jenssen and Ljungberg.[7] In the present study, CGR was estimated only for specimens in which through-wall IG crack had been confirmed by SEM

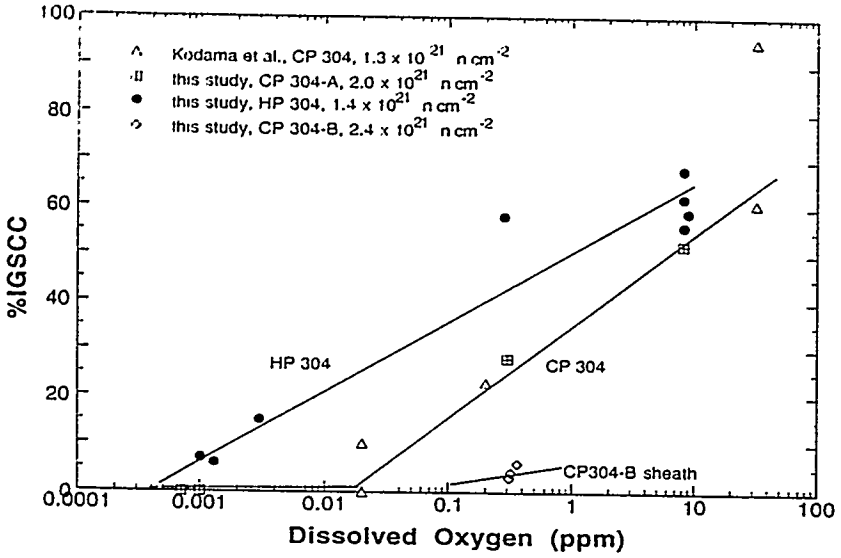

Figure 2.

Comparison of %IGSCC vs. DO of high- and commercial-purity Type 304 SS neutron absorber tubes (this study) and commercial-purity Type 304 SS dry tubes (Kodama et al.).

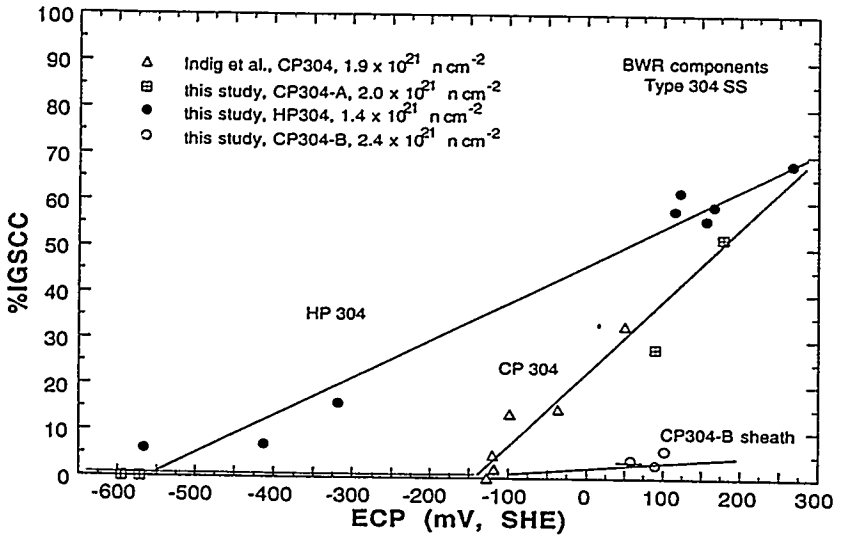

Figure 3.

Comparison of %IGSCC vs. ECP of high- and commercial-purity Type 304 SS neutron absorber tubes (this study) and commercial-purity Type 304 SS BWR sheet component (Indig et al.).

fractography. For such specimens, the depth and time of IG cracking can be determined fairly accurately from the fracture-surface map and load-elongation curve, respectively. The estimated CGRs determined in this way are plotted as a function of ECP in Fig. 4. Also shown in the figure are similar results reported by Jenssen and Ljungberg[7] and CGRs calculated from the SSRT and constant-load test data reported by Kodama et al.[4,9] and Katsura et al.,[12] respectively.

Results in Fig. 4 indicate that IGCGRs determined from SSRT and constant-load tests on actual BWR components are similar for similar range of fluence and ECP. However, these rates obtained from BWR components are significantly higher than those obtained from the rod-shaped SSRT specimens of Jenssen and Ljungberg.[7] Strain rate was significantly different in these tests, ranging from 5×10^{-8} s^{-1} to 2.5×10^{-7} s^{-1}. It is not clear if crack growth rates determined from actual reactor components are influenced significantly by the component fabrication variables and differences in irradiation conditions. However, test parameters such as stress intensity and strain rate should influence CGR significantly. Stress intensity is not likely to have been comparable for the SSRT and constant-load tests examined in Fig. 4. A more accurate comparison would be possible if CGRs were measured under conditions of constant stress intensity.

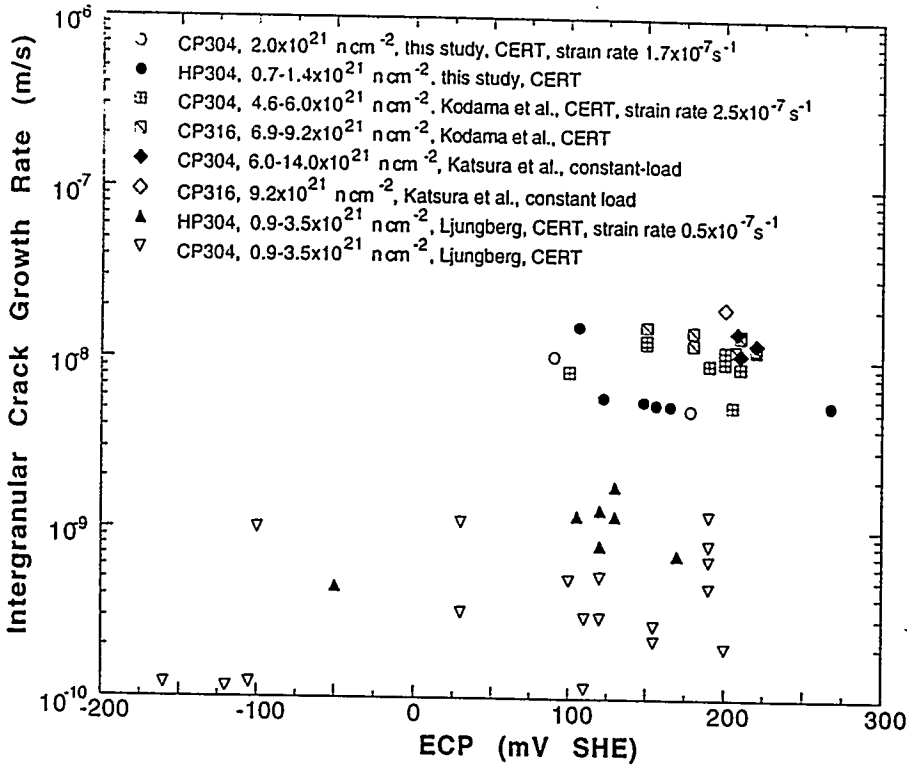

Figure 4. Intergranular crack growth rate vs. ECP determined from constant-extension-rate and constant-load tests on BWR tube components and rod-tensile specimens irradiated in BWR.

Discussion

Threshold ECP. Although the threshold ECP of <–140 mV SHE to suppress IASCC in the CP materials was confirmed to agree well with that reported by Indig et al.,[3] the contrasting dependence of susceptibility to intergranular stress corrosion cracking (IGSCC) of the HP and CP materials on water chemistry (DO and ECP) was unexpected. To obtain a better understanding of the peculiar behavior of the HP tubes, grain-boundary microchemistry has been analyzed by Auger electron spectroscopy (AES). The results, some of which have been reported elsewhere,[5,6,14] are summarized in Fig. 5.

Role of Cr Depletion. The HP-grade neutron absorber tubes are characterized by more pronounced grain-boundary Cr depletion than that in the CP-grade absorber tubes or sheath. This is shown in Fig. 5A, in which %IGSCC of the three types of BWR components irradiated to a comparable fluence level of 1.4 x 10^{21} n cm^{-2} to 2.4 x 10^{21} n cm^{-2} has been plotted as a function of grain-boundary Cr concentration. The lower grain-boundary Cr concentration in the HP materials is believed to be associated with the relatively higher susceptibility of the materials to IASCC. However, it is difficult to explain the contrasting behavior of the HP and CP materials to water chemistry solely on the basis of grain-boundary Cr depletion. Likewise, it is also difficult to explain some of the important and well-known characteristics of IASCC on the basis of a premise that grain-boundary depletion of Cr plays a primary role, e.g., strong heat-to-heat variation in susceptibility among heats of virtually identical chemical composition[10] and the significant cracking susceptibility observed after irradiation at such low temperatures as ≈50[13] and ≈200°C.[8]

Role of Ni. Higher Ni concentration on grain boundaries appears to be conducive to suppression of IASCC susceptibility (Fig. 5B). This is qualitatively consistent with similar

observation reported by Cookson et al.[8] It seems that lower Ni concentration tends to increase metastability of grain boundaries in austenitic stainless steels.

Role of Li and B. The results in Fig. 5C show that %IGSCC correlates well with intensities of Auger electrons that give rise to a characteristic peak at 58 eV (i.e., secondary peaks of Ni and Li). The origin of the peak, which exhibited a characteristic shape similar to that of Li but different from that of Ni, was examined extensively in a previous report.[6] From the examination, it was concluded that at least some portion of the peak height was produced as a result of Li impurity contained in the irradiated BWR components. Therefore, the results of Figs. 5B and 5C indicate that higher concentrations of Ni and Li, and hence B, are beneficial in suppressing IASCC.

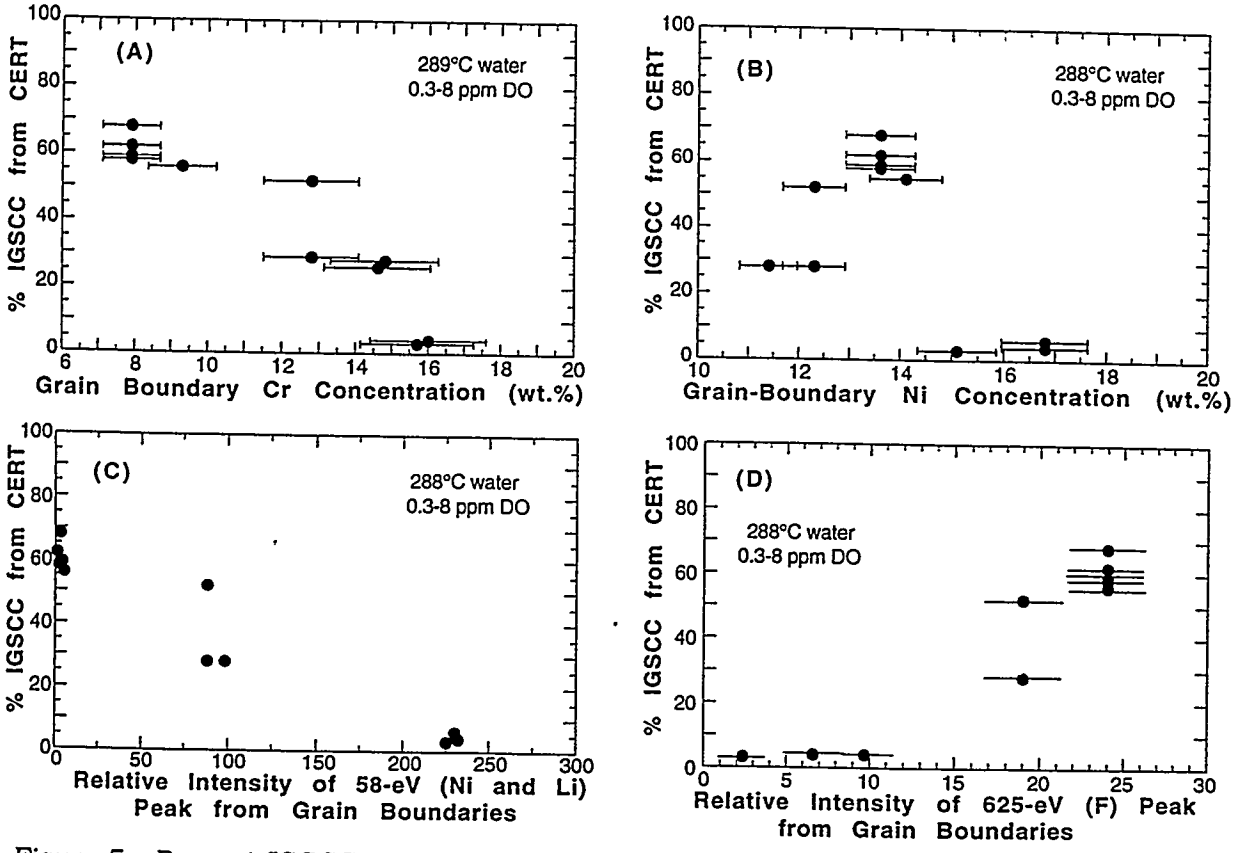

Figure 5. Percent IGSCC vs. grain-boundary concentration of Cr (A) and Ni (B); and vs. relative intensities of Auger electrons with characteristic energies of (C) 58-eV (Ni plus Li) and (D) 625-eV (F), measured on grain boundaries in the BWR components that were irradiated to 1.4 to 2.4 x 10^{21} n cm^{-2}.

Role of N. We have reported evidence of grain-boundary segregation of N in neutron absorber tubes fabricated from two heats of the HP material (i.e., HP304-A and -CD) that were tested in this study.[6] Therefore, a higher concentration of N on grain boundaries seems to be deleterious to resistance to IASCC, a finding consistent to that reported by Kasahara et al.[11]

Role of F. The results shown in Fig. 5D indicate that a relatively higher level of F on grain boundaries in HP absorber tubes (higher than in the CP tubes or sheath) is associated with higher susceptibilities to IASCC.[14] Inadvertent contamination of reactor components by fluorine is believed to be associated primarily with pickling (in a solution containing HF) in the case of tubular components, and with the use of F-containing weld flux in the case of large welded components such as BWR core shrouds and certain older top guides.[14]

The results in Fig. 5D on the effect of F appears to be consistent with the effect of F ions dissolved in water on the stress corrosion cracking of nonirradiated sensitized stainless

steel, which was reported by Ward et al.[15] In that study, F ions as low as ≤ 1 ppm in water produced intergranular cracking to varying degrees in sensitized Type 304, 316, and 348 SS. Besides thermal sensitization, at least one of the following conditions were found to be prerequisite for the intergranular attack in the nonirradiated materials: (1) tensile stress (applied or residual), (2) cold work, (3) a crevice, or (4) visible oxide film.

DO and ECP Dependences of HP Tubes. Ward et al.[15] also reported observation of accelerated IGSCC of nonirradiated thermally sensitized bend specimens or weldments of CP-grade Type 304 SS that were contaminated with F. Similar to the observation of Ward et al., the IASCC-resistant CP sheath was characterized by negligible grain-boundary Cr depletion and absence of F. On the other hand, the IASCC-susceptible HP absorber tubes were characterized by significant grain-boundary Cr depletion and relatively high level of F (Figs. 5A and 5D). It appears very likely that a small amount of F contamination in the HP absorber tubes is sufficient to accelerate cracking along grain boundaries significantly depleted of Cr. Similar to the dependences of the HP neutron absorber tubes to DO and ECP observed in the present investigation, Ward et al. reported that F-assisted IGSCC was less sensitive to DO than was classical IGSCC of thermally sensitized F-free specimens.[15] However, a mechanistic understanding of the F-assisted intergranular cracking and the strong influence of grain-boundary Cr depletion (via either thermal sensitization or irradiation-induced process) have remained unexplained.

Model of F-Assisted Cracking. The catalytic role of halide impurities in accelerating aqueous corrosion of Fe and Fe-based alloys is known to be strongly influenced by concentration of Cr ions in water.[16] The corrosion acceleration has been attributed to the orders-of-magnitude faster rate of formation of a ligand complex between Fe-halide (i.e., halide anion chemisorbed on Fe adsorbent) and H_2O molecules than the rate of formation of a similar ligand complex between halide-free Fe atom and H_2O molecules.[16] A similar effect can be postulated for relative reaction rates to form F-containing and F-free ligand complexes of $FeF(H_2O)_5$ and $Fe(H_2O)_6$, respectively. Halide atom is released from the labile ligand complex [e.g., $FeF(H_2O)_5$] dissolved in water when H_2O replaces the halide atom in the complex, thus leading to a classical catalytic role by halides. However, this reaction chain is broken when the concentration of Cr ions in water is high (e.g., in the crack tip at grain boundaries of relatively insignificant Cr depletion), because the Cr-halide-H_2O ligand complex [e.g., $CrF(H_2O)_5$] is formed rapidly but remains inert in water, thereby preventing a catalytic role of the halide atoms (e.g., F atoms) According to this model, key factors that influence susceptibility to IASCC will be (1) concentration of free (i.e., not trapped by stable precipitates[14] or compounds) halide atoms (e.g., F) available on grain boundaries, (2) concentration of Cr ions in the crack tip, and (3) lability of the $FeF_x(H_2O)_y$ complex under irradiation in LWR water.

The above model seems consistent with not only the behaviors of HP-grade neutron-absorber tubes (high susceptibility) and CP-grade control blade sheath (negligible susceptibility) observed in this work, but also with the increased susceptibility to IGSCC of F-contaminated welds of either nonirradiated or irradiated Type 304 SS. The model also predicts that, in the absence of an appreciable concentration of Cr ions in water (at very low ECP), a low concentration of F in steels can sustain the catalytic role in the stagnant environment of the slowly advancing crack tip. Fractographic examination of the cracked HP absorber tubes by stereo SEM revealed that rugged fracture surfaces have a depth as great as ≈20 grains in some regions in the direction perpendicular to the crack propagation. At such a rugged crack tip, in which surface-to-volume ratio (of water) is very high, it is more likely that F ions in water will exist in concentrations sufficiently high to sustain the catalytic reaction.

Conclusions

(1) Effects of dissolved oxygen (DO) and electrochemical potential (ECP) on susceptibility of commercial-purity (CP) Type 304 stainless steel (SS) BWR neutron absorber tubes to IASCC, determined from slow-strain-rate tensile tests in simulated BWR water at 289°C, were similar to those of other CP-grade Type 304 SS BWR components reported in a previous investigation. Threshold ECP and DO to protect the CP-grade materials against susceptibility to IASCC were confirmed to be, respectively,

<-140 mV SHE and <0.01 ppm. For fluence >1.3 x 10^{21} n cm^{-2}, susceptibility to IASCC seems to be determined primarily by DO or ECP, indicating the dominant effect of water chemistry and the secondary effect of fluence.

(2) Dependence of IASCC susceptibility of BWR components fabricated from high-purity (HP) heats of Type 304 SS differed from those of the components fabricated from CP materials. In comparison to the CP heats, susceptibility of the HP heats was less dependent on water chemistry (DO and ECP) and was significantly higher regardless of water chemistry and fluence.

(3) The HP-grade neutron absorber tubes, significantly more susceptible to IASCC than were the CP tubes or sheaths, were characterized by lower concentrations of Cr, Ni, and Li and higher concentrations of F and N on grain boundaries than those of the CP-grade components, indicating that higher levels of Cr, Ni, and B and lower levels of F and N in steels are beneficial in suppressing IASCC. Although it is not clear at this time as to the specific culprit elements and the exact metallurgical processes that play the most important role, the higher susceptibility and its dependence on water chemistry of the HP tubes can be explained well by a model based on a synergism between grain-boundary Cr depletion and F contamination (most likely associated with component fabrication) in which F atoms play a catalytic role leading to accelerated IGSCC.

(4) Intergranular crack growth rates estimated from the present SSRT and constant-load tests conducted on BWR components in other laboratories are similar but significantly higher than those estimated from the SSRT data reported for BWR-irradiated test specimens. Origin of the discrepancy is not clear at this time, although factors such as stress intensity and strain rate are suspected.

Acknowledgments

The authors are grateful to D. R. Perkins for his experimental contributions. The irradiated specimens from BWR components were obtained through the kind assistance of Drs. A. J. Jacobs, L. Nelson, and R. Kohli. The authors also thank Drs. M. McNeil and W. J. Shack for helpful comments.

References

1. P. L. Andresen and F. P. Ford, Corrosion/95, Paper No. 419 (Houston, TX, National Association of Corrosion Engineers, 1995).
2. A. J. Jacobs, G. P. Wozadlo, K. Nakata, T. Yoshida, and I. Masaoka, Proc. 3rd Int. Symp. Environmental Degradation of Materials in Nuclear Power Systems – Water Reactors, G. J. Theus and J. R. Weeks, eds., The Metallurgical Society, Warrendale, PA, p. 673 (1988).
3. M. E. Indig, J. L. Nelson, and G. P. Wozadlo, Proc. 5th Int. Symp. on Environmental Degradation of Materials in Nuclear Power Systems – Water Reactors, D. Cubicciotti, E. P. Simonen, and R. Gold, eds., American Nuclear Society, La Grange Park, IL, p. 941 (1992).
4. M. Kodama, S. Nishimura, J. Morisawa, S. Shima, S. Suzuki, and M. Yamamoto, ibid., p. 948.
5. H. M. Chung, W. E. Ruther, J. E. Sanecki, A. G. Hins, and T. F. Kassner, Effects of Radiation on Materials: 16th Int. Symp., ASTM STP 1175, A. S. Kumar, D. S. Gelles, R. K. Nanstad, and T. A. Little, eds., American Society for Testing and Materials, Philadelphia, p. 851 (1993).
6. H. M. Chung, W. E. Ruther, J. E. Sanecki, and T. F. Kassner, Proc. 6th Intl. Symp. on Environmental Degradation of Materials in Nuclear Power Systems - Water Reactors, R. E. Gold and E. P. Simonen, eds., The Minerals, Metals, and Materials Society, Warrendale, PA, p. 511 (1993).
7. A. Jenssen and L. G. Ljungberg, ibid., p. 547.
8. J. M. Cookson, D. L. Damcott, G. S. Was, and P. L. Anderson, ibid., p. 573.

9. M. Kodama, R. Katsura, J. Morisawa, S. Nishimura, S. Suzuki, K. Asano, K. Fukuya, and K. Nakata, ibid., p. 583.

10. F. Garzarolli, P. Dewes, R. Hahn, and J. L. Nelson, ibid., p. 607.

11. S. Kasahara, K. Nakata, K. Fukuya, S. Shima, A. J. Jacobs, G. P. Wozadlo, and S. Suzuki, ibid., p. 615.

12. R. Katsura, J. Morisawa, M. Kodama, S. Nishimura, S. Suzuki, S. Shima, and M. Yamamoto, ibid., p. 625.

13. M. Kodama, J. Morisawa, S. Nishimura, K. Asano, S. Shima, and K. Nakata, J. Nucl. Mater., 212–215 (1994), p. 1509.

14. H. M. Chung, W. E. Ruther, and J. E. Sanecki, "Role of Trace Elements in SCC of Irradiated Austenitic Stainless Steels," in Environmentally Assisted Cracking in Light Water Reactors: Semiannual Report, October 1993–March 1994, NUREG/CR-4667, ANL-95/2, Vol. 18, March 1995, Argonne National Laboratory, pp. 27–35.

15. C. T. Ward, D. L. Mathis, and R. W. Staehle, Corrosion, 25 (1969), p. 394.

16. N. C. Huang and Z. Nagy, J. Electrochem. Soc., 134 (1987), p. 2215.